X-Rays Writing/Reading of Charge Density Waves in the CuO$_2$ Plane of a Simple Cuprate Superconductor

Gaetano Campi [1,*] [ID], **Alessandro Ricci** [2], **Nicola Poccia** [3], **Michela Fratini** [4] and **Antonio Bianconi** [1,5] [ID]

1   Institute of Crystallography, CNR, Monterotondo, 00015 Roma, Italy
2   Deutsches Elektronen-Synchrotron DESY, 22607 Hamburg, Germany; phd.alessandro.ricci@gmail.com
3   Department of Physics, Harvard University, Cambridge, MA 02138, USA; npoccia@g.harvard.edu
4   Fondazione Santa Lucia I.R.C.C.S., 00179 Roma, Italy; michela.fratini@gmail.com
5   Rome International Center of Materials Science (RICMASS), 00185 Roma, Italy;
    antonio.bianconi@ricmass.eu
*   Correspondence: gaetano.campi@ic.cnr.it; Tel.: +39-06-9067-2624

Abstract: It is now well established that superconductivity in cuprates competes with charge modulations giving an electronic phase separation at nanoscale. More specifically, superconducting electronic current takes root in the available free space left by electronic charge ordered domains, called charge density wave (CDW) puddles. This means that CDW domain arrangement plays a fundamental role in the mechanism of high temperature superconductivity in cuprates. Here we report about the possibility of controlling the population and spatial organization of the charge density wave puddles in a single crystal La$_2$CuO$_{4+y}$ through X-ray illumination and thermal treatments. We apply a pump-probe method—based on *X-ray illumination* as a pump and X-ray diffraction as a probe—setting a *writing/reading* procedure of CDW puddles. Our findings are expected to allow new routes for advanced design and manipulation of superconducting pathways in new electronics.

1. Introduction

The nano-electronics for new generations of devices made of complex modern materials are extremely sensitive to changes in defect disposition [1–3]. To control defect complexity in superconductors, some experimental approaches have been proposed. The manipulation of an array of superconducting grains has been found to be possible by either controlling defects self-organization using scanning tips [4] or using external stimulus [5–9]. Recently, the improvement of film deposition techniques has allowed the production of artificial superconducting puddles embedded in a 2D layer intercalated by different block layers in a layered material [10–13]. Although it is common knowledge that a suspended two-dimensional layer should be thermodynamically unstable, and therefore should not exist in nature [14], new advanced materials such as two-dimensional graphene have recently challenged this paradigm [15–17]. In this material, electronic properties are affected by curved geometries originating from topological defects such as dislocations or ripples.

High temperature superconductors (HTS) are hetero-structures, at their atomic limit, made of intercalated two-dimensional layers. Like graphene, CuO$_2$ layers (with the structure of the 110 plane of a body centered cubic (bcc) lattice) in cuprates [18,19], as well as boron (B) layers in diborides [20–22] or FeSe layers in A$_x$Fe$_{2-y}$Se$_2$ chalcogenides [23] are truly two-dimensional crystals (just one atom thick). Because of their general instability with respect to bending fluctuations, these conductive planes are rippled and these effects are enormously relevant for their structural, thermodynamic, and electronic

properties. Using strain engineering it is possible to modify in a desirable way the electronic structure of atomic layers with exciting perspectives for electronics. In case of HTS, electronic organization in modulated structures called *charge density waves* (CDWs) have been found to play an essential role in superconducting mechanisms [24–27]. In fact, it has been established that electronic superconducting currents develop in the space free from CDWs [28,29]. In this framework, the possibility of controlling both the population and the spatial arrangement of the CDW puddles becomes a key point to be investigated for different possible applications.

CDWs in cuprates have been found recently through the real space visualization of the 3D superlattices measured by scanning micro X-ray diffraction in different single crystals [8,9,18,23,28–30]. These transverse modulations are similar to those found in the superconducting Bi2212, characterized by the wave-vectors 0.21**b*** [31,32]. They are due to stripes with a period of 4.8b along the diagonal direction **b**. It has been found that the CDW puddles are spatially anti-correlated with other spin and charge ordered puddles and with domains rich with interstitial dopant oxygen defects [28,33–36] in a scenario of frustrated phase separation which is a common feature of doped cuprates [37–41]. Either oxygen interstitial-rich domains or CDW puddles are sensitive to X-ray illumination in a different temperature range [42,43] but together they work to establish the optimum inhomogeneity, which raises the critical temperature to the optimum value [18]. Here we study CDW puddles in an oxygen doped orthorhombic La_2CuO_{4+y} (LCO) superconductor showing the details of the manipulation process, which allow tuning of the order of the CDW puddles in the LCO system.

2. Materials and Methods

Diffraction measurements on a single crystal of underdoped La_2CuO_{4+y} of size $3 \times 2 \times 0.5$ mm^3, were performed on the crystallography beamline, XRD1, at ELETTRA, Trieste, Italy [44]. The sample was grown first as La_2CuO_4 by flux method and then doped by electrochemical oxidation. The X-ray beam, emitted by the wiggler source of the 2 GeV electron storage ring, was monochromatized by a Si(111) double crystal, and focused on the sample. The superconducting transitions of samples have been established using contactless single-coil inductance as described elsewhere [5,16,30]. The temperature of the crystal was monitored with an accuracy of ±1 K. We have collected the data in the reflection geometry using a charge coupled device (CCD) detector, a photon energy of 12.4 KeV (wavelength $\lambda = 1$ Å). The sample oscillation around the crystal *b*-axis was in a range $0 < \Phi < 20°$, where Φ is the angle between the direction of the photon beam and the crystal *a*-axis. We have investigated a portion of the reciprocal space up to 0.6 Å^{-1} momentum transfer, i.e., recording the diffraction spots up to the maximum indexes h = 3, k = 3, and l = 19 in the **a***, **b***, and **c*** directions of reciprocal space, respectively. Thanks to the high brilliance source, it has been possible to record a large number of weak superstructure spots around the main peaks of the average structure. Twinning of the crystal has been taken into account to index the superstructure peaks. The orthorhombic lattice parameters of single crystal were determined to be $a = (5.386 \pm 0.004)$ Å, $b = (5.345 \pm 0.008)$ Å, $c = (13.205 \pm 0.031)$ Å at room temperature. The space group of the sample is *Fmmm*.

## 3. Results

3.1. Temperature Dependence of CDW Puddles

Indexing of superlattice peaks around the Bragg lattice reflections shows the presence of incommensurate CDW modulation with wave-vector $\mathbf{q_{CDW}}$ = (0.023**a*** + 0.21**b*** + 0.29**c***) where **a***, **b***, and **c*** are the unit vectors of the orthorhombic reciprocal lattice. The profiles of this superstructure peak, measured at 300 K and 100 K in the *a**–*b** plane and fitted by Gaussian line shape, are shown in Figure 1a,b.
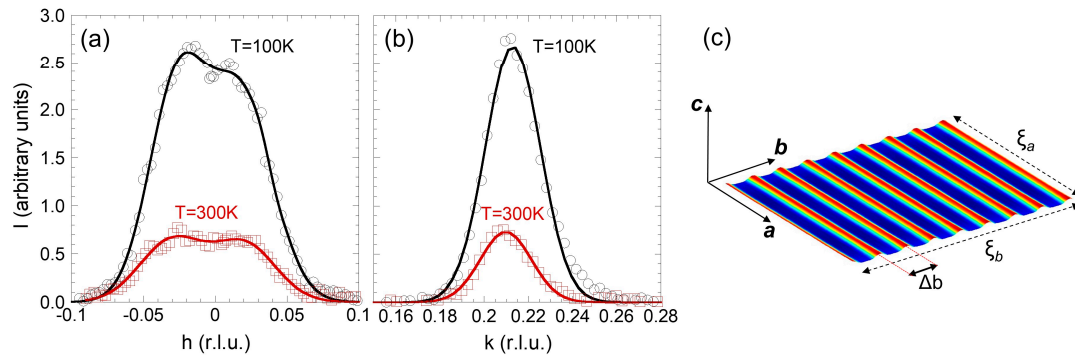
Figure 1. Profiles of the **q$_{CDW}$** superstructure along the (**a**) **a*** and (**b**) **b*** directions. The profiles, measured around the 006 Bragg peak, have been fitted by Gaussian lineshape (continuous lines). The peaks along the **a*** direction show quite diffuse scattering covering a larger h-range around zero. (**c**) A typical single charge density waves (CDW) puddle in La$_2$CuO$_{4+y}$ in the *a–b* plane with size of $\xi_a \times \xi_b$. Δb represents the period of the CDW, corresponding to 4.76 unit cells along the crystal *b*-axis. **a**, **b**, and **c** represent the orthogonal directions of the orthorhombic lattice.

The modulations along **a*** give X-ray diffuse superlattice peaks due to a quasi one-dimensional (1D) modulation associated with stripes running in the **a** direction with a period of about 2.6 nm in the **b** direction where **a**, and **b** represent the unit vectors of the orthorhombic lattice. These incommensurate charge density waves (CDWs) are established in nanoscale regions, as shown by the analysis of the widths of X-ray satellites. Indeed, the full width at half-maximum (FWHM) of the CDW peaks, along the **a*** and along the **b*** direction, are related with the correlation length of the CDW puddles $\xi_a = a/\text{FWHM}(\textbf{a*})$ and $\xi_b = b/\text{FWHM}(\textbf{b*})$. We have found 11 ± 2 nm and 19 ± 2 nm for ξ_a and ξ_b, respectively. A pictorial view of the **q$_{CDW}$** modulation is given in Figure 1c.

The temperature dependence of the CDW order is shown in Figure 2.
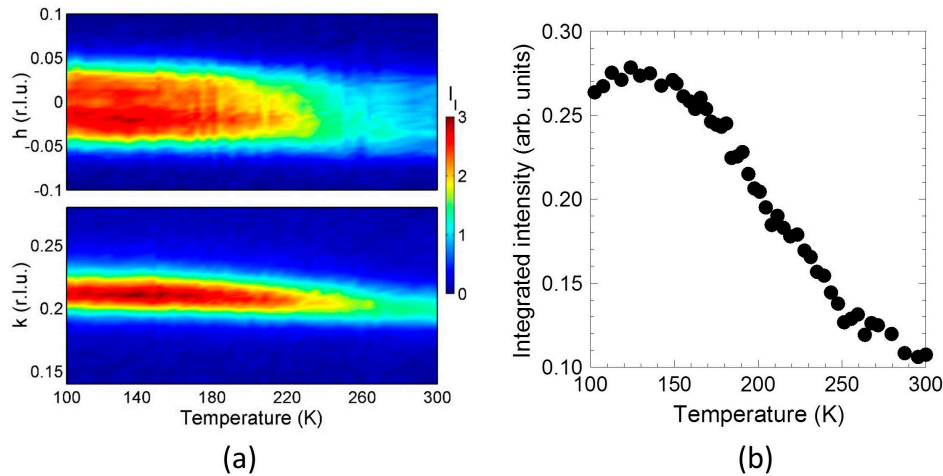
Figure 2. (**a**) Map of normalized diffraction profiles **q$_{CDW}$** along (upper panel) **a*** and (lower panel) **b*** directions during cooling from room temperature down to *T* = 100 K. (**b**) Integrated intensity of the **q$_{CDW}$** peak during the cooling.

The normalized profiles along the **a*** and **b*** directions are visualized by upper and lower panel in Figure 2a, respectively. The integrated intensity of the CDW peak increases by cooling the sample from room temperature down to 100 K, as shown in Figure 2b. We find a CDW onset temperature of 250 K.

3.2. Controlling CDW Puddles by X-ray Illumination

The possibility of photo generating CDW puddles in La_2CuO_{4+y} has been previously shown in [18]. Our pump and probe experimental approach, based on X-ray illumination and diffraction, has been performed with synchrotron X-ray photons focused onto a spot size of 100 μm^2 on the sample surface.

We have found that the effect of photo generation of CDW in the X-ray energy ranges between 8 KeV and 12 KeV and does not depend on photon energy but on the X-ray illumination fluence. Furthermore, new measurements are required to investigate the pump and probe process in the soft X-ray and optical regimes. The photon flux (defined as the number of photons hitting the sample surface per second per unit area) is given by $\Phi_{P(0.1nm)} = 5 \times 10^{14} N_{P(0.1nm)}$ $s^{-1}cm^{-2}$ and corresponds to the power density of 1 W·cm^{-2}. In our method, the X-ray photon beam works at the same time as the pump and probe on a surface layer with an area of 100 μm^2 and about 1.5 μm thick. In this volume, the physical state of the system is controlled by the fluence $F_{P(0.1nm)}(N_{P(0.1nm)}$ cm$^{-2}) = \Phi_P \cdot t$.

We quenched the sample from room temperature, where CDW puddle population is weak, down to 100 K, leading the system to a frozen metastable disordered state. Then we illuminated the sample continuously. The pump and probe results are illustrated in Figure 3.
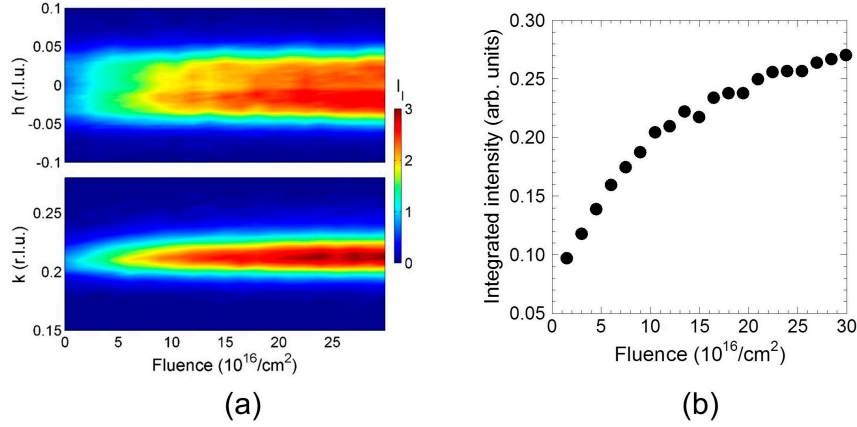
Figure 3. (**a**) Map of normalized diffraction profiles **q**$_{CDW}$ along (upper panel) **a*** and (lower panel) **b*** direction during the X-ray continuous illumination at T = 100 K. (**b**) Integrated intensity of the **q**$_{CDW}$ peak increases by a factor of ~3 during the illumination.

The color maps obtained from the normalized profiles, of **q**$_{CDW}$(**a***) and **q**$_{CDW}$(**b***) shown in the upper and lower panels of Figure 3a, respectively, visualize the evolution of CDW during the X-ray illumination. The CDW peak integrated intensity increases by about three times under illumination, as shown by the integrated intensity of **q**$_{CDW}$ peak in Figure 3b.

A single oscillation in each puddle is given by $\gamma_b = b/q_{CDW}(b^*) = 2.5$ nm and $\gamma_a = a/ q_{CDW}(a^*) = 23.4$ nm along the **b** and **a** direction, respectively; here $q_{CDW}(b^*)$ and $q_{CDW}(a^*)$ are the components of **q**$_{CDW}$ along the **a*** and **b*** directions. Each puddle contains a number of oscillations given by $\xi_a/\gamma_a = 0.4$ and $\xi_b/\gamma_b = 7$ in the **a** and **b** directions, respectively. Thus, we have $\xi_a \times \xi_b$ puddles made of about seven unidirectional stripes each. A pictorial view of CDW puddles is shown in the upper part of Figure 4.

3.3. CDW Writing/Reading Procedure

Thus, we have shown the feasibility of tuning the CDW population through X-ray illumination and also the possibility to erase such order by thermal treatments. These are the elementary steps for a writing/reading process. We have therefore performed a series of experiments of direct manipulation of the CDW puddles in real space in a La_2CuO_{4+y} sample through local X-ray continuous illumination at low temperatures.

Figure 4a shows the color-map of the intensity of the CDW peak, along **b***, obtained by scanning the sample using an X-ray beam of 100 μm^2 and a low fluence of 1.5 (10^{16} cm^{-2}). The histogram in Figure 4c shows a quite flat distribution of the CDW intensity, but not zero. In fact, in order to have successful X-ray illumination growth of the CDW puddles, the region being irradiated must already have some seeds of CDW puddles, as shown by the light blue stripe in the map center of Figure 4a.
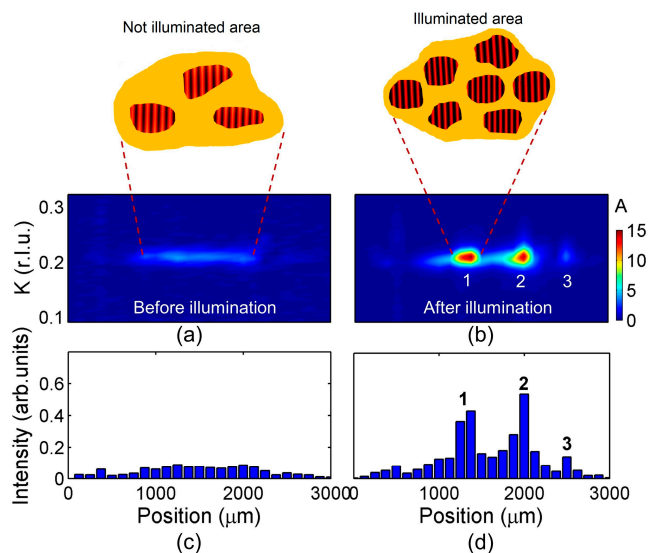
Figure 4. Writing/reading local CDW rich puddles domains by X-ray illumination. Diffraction scanning profiles along the sample (**a**) before and (**b**) after X-ray illumination by a 100 micron size beam in the points indicated with 1, 2, and 3. Scanning profile integral area (**c**) before and (**d**) after X-ray illumination.

We irradiated three spots indicated by 1, 2, and 3 using an X-ray beam of 100 μm^2 for a total fluence of 50 (10^{16} cm^{-2}); the effects of this continuous local illumination are than monitored by re-scanning the sample using the low fluence of 1.5 (10^{16} cm^{-2}). The results are shown in the map of Figure 4b by the 3 bright spots at the positions 1, 2, and 3 of increased integral intensity, respectively shown also in the histogram of Figure 4d.

4. Discussion

The relevance of the possibility of controlling and manipulating the spatial organization of CDW puddles populations lies in the fact that the free electrons form superconducting currents flowing in the interstitial space [28,29]. Thus, changing the population of the CDW puddles *point by point* leads to modifying the interstitial space available for the electron currents. In atomic layers, intrinsic thermodynamic instabilities give rise to charge (spin, orbital) ordering phenomena. Easy methods—such as thermal cycling and X-ray continuous illumination with focused beams—can write, read, and erase arbitrary CDW pathways. This will enable the design of new devices with controlled functionality.

5. Conclusions

In conclusion, in this paper we reported on the study of CDWs in an orthorhombic crystal La$_2$CuO$_{4+y}$ where dopants are mobile oxygen interstitials. The CDWs in this compound has unique features in comparison with CDWs in different cuprate families [45–48]: the CDW wave-vector has been found to be aligned along the *b* orthorhombic axis in the diagonal direction from the Cu-O-Cu direction like in nikelates, cobaltates, and in the doped La124 family at very low doping. The photo-stimulated CDW puddles in La$_2$CuO$_{4+y}$ are uniaxial and form a smectic phase in the crystal while in underdoped YBa$_2$Cu$_3$O$_{6+y}$ and Hg1201 form a nematic phase. Moreover, the average CDW puddles are formed by

only seven oscillations which is larger than in Hg1201, but smaller than in other systems. These results support the increasing accumulating experimental evidence that the CDW character in cuprates changes in different families [45–48]. We have shown the details of the manipulation process which allow tuning of the order of the CDW puddles in the Lanthanum Copper Oxide system. This approach has unveiled the condition and the process of formation of charge density waves puddles in the CuO_2 plane and shows a possible method for their direct control. In particular, we have shown that the synthesis of photo-stimulated CDW puddles in the LCO can be controlled by setting the fluence of synchrotron X-ray illumination and thermal cycling. Thanks to advanced X-ray optics, it will be possible to write and read CDW pathways whose size is determined by the X-ray beam size. This new approach in arbitrary nanostructures manipulation promises increasingly large-scale integration of conventional devices.

Author Contributions: G.C. and A.B. conceived and designed the experiments; G.C. and M.F. performed the experiments; G.C., A.R., and M.F. analyzed the data; G.C., N.P., and A.B. wrote the paper.

Conflicts of Interest: The authors declare no conflict of interest.

References

1. Littlewood, P. Superconductivity: An X-ray oxygen regulator. *Nat. Mater.* **2011**, *10*, 726–727. [CrossRef] [PubMed]

2. Awschalom, D.D.; Bassett, L.C.; Dzurak, A.S.; Hu, E.L.; Petta, J.R. Quantum Spintronics: Engineering and Manipulating Atom-Like Spins in Semiconductors. *Science* **2013**, *339*, 1174–1179. [CrossRef] [PubMed]

3. Bryant, B.; Renner, C.; Tokunaga, Y.; Tokura, Y.; Aeppli, G. Imaging oxygen defects and their motion at a manganite surface. *Nat. Commun.* **2011**, *2*, 212. [CrossRef] [PubMed]

4. Custance, O.; Perez, R.; Morita, S. Atomic force microscopy as a tool for atom manipulation. *Nat. Nanotechnol.* **2009**, *4*, 803–810. [CrossRef] [PubMed]

5. Poccia, N.; Fratini, M.; Ricci, A.; Campi, G.; Barba, L.; Vittorini-Orgeas, A.; Bianconi, G.; Aeppli, G.; Bianconi, A. Evolution and control of oxygen order in a cuprate superconductor. *Nat. Mater.* **2011**, *10*, 733–736. [CrossRef] [PubMed]

6. Garganourakis, M.; Scagnoli, V.; Huang, S.W.; Staub, U.; Wadati, H.; Nakamura, M.; Guzenko, V.A.; Kawasaki, M.; Tokura, Y. Imprinting Magnetic Information in Manganites with X Rays. *Phys. Rev. Lett.* **2012**, *109*. [CrossRef] [PubMed]

7. Poccia, N.; Bianconi, A.; Campi, G.; Fratini, M.; Ricci, A. Size evolution of the oxygen interstitial nanowires in La_2CuO_{4+y} by thermal treatments and X-ray continuous illumination. *Superconduct. Sci. Technol.* **2012**, *25*. [CrossRef]

8. Ricci, A.; Poccia, N.; Campi, G.; Coneri, F.; Barba, L.; Arrighetti, G.; Polentarutti, M.; Burghammer, M.; Sprung, M.; v Zimmermann, M.; et al. Networks of superconducting nano-puddles in 1/8 doped $YBa_2Cu_3O_{6.5}$ controlled by thermal manipulation. *New J. Phys.* **2014**, *16*. [CrossRef]

9. Campi, G.; Ricci, A.; Poccia, N.; Barba, L.; Arrighetti, G.; Burghammer, M.; Caporale, A.S.; Bianconi, A. Scanning micro-X-ray diffraction unveils the distribution of oxygen chain nanoscale puddles in $YBa_2Cu_3O_{6.33}$. *Phys. Rev. B* **2013**, *87*. [CrossRef]

10. Hilgenkamp, H.; Mannhart, J. Grain boundaries in high-T_c superconductors. *Rev. Mod. Phys.* **2002**, *74*, 485–549. [CrossRef]

11. Zubko, P.; Gariglio, S.; Gabay, M.; Ghosez, P.; Triscone, J.M. Interface physics in complex oxide heterostructures. *Annu. Rev. Condens. Matter Phys.* **2011**, *2*, 141–165. [CrossRef]

12. Mannhart, J.; Schlom, D.G. Oxide interfaces—An opportunity for electronics. *Science* **2010**, *327*, 1607–1611. [CrossRef] [PubMed]

13. Hwang, H.Y.; Iwasa, Y.; Kawasaki, M.; Keimer, B.; Nagaosa, N.; Tokura, Y. Emergent phenomena at oxide interfaces. *Nat. Mater.* **2012**, *11*, 103–113. [CrossRef] [PubMed]

14. Mermin, N.D. Crystalline order in two dimensions. *Phys. Rev.* **1968**, *176*, 250–254. [CrossRef]

15. Geim, A.K.; Novoselov, K.S. The rise of graphene. *Nat. Mater.* **2007**, *6*, 183–191. [CrossRef] [PubMed]

16. Fasolino, A.; Los, J.H.; Katsnelson, M.I. Intrinsic ripples in graphene. *Nat. Mater.* **2007**, *6*, 858–861. [CrossRef] [PubMed]

17. Bao, W.; Miao, F.; Chen, Z.; Zhang, H.; Jang, W.; Dames, C.; Lau, C.N. Controlled ripple texturing of suspended graphene and ultrathin graphite membranes. *Nat. Nanotechnol.* **2009**, *4*, 562–566. [CrossRef] [PubMed]

18. Poccia, N.; Ricci, A.; Campi, G.; Fratini, M.; Puri, A.; Di Gioacchino, D.; Marcelli, A.; Reynolds, M.; Burghammer, M.; Saini, N.L.; et al. Optimum inhomogeneity of local lattice distortions in La_2CuO_{4+y}. *Proc. Natl. Acad. Sci. USA* **2012**, *109*, 15685–15690. [CrossRef] [PubMed]

19. Saini, N.L.; Oyanagi, H.; Ito, T.; Scagnoli, V.; Filippi, M.; Agrestini, S.; Campi, G.; Oka, K.; Bianconi, A. Temperature dependent local Cu-O displacements from underdoped to overdoped La-Sr-Cu-O superconductor. *Eur. Phys. J. B* **2003**, *36*, 75–80. [CrossRef]

20. Campi, G.; Cappelluti, E.; Proffen, T.; Qiu, X.; Bozin, E.S.; Billinge, S.; Agrestini, N.; Saini, L.; Bianconi, A. Study of temperature dependent atomic correlations in MgB_2. *Eur. Phys. J. B* **2006**, *52*, 15–21. [CrossRef]

21. Campi, G.; Ricci, A.; Bianconi, A. Local structure in $Mg_{1-x}Al_xB_2$ system by high resolution neutron diffraction. *J. Supercond. Nov. Magn.* **2012**, *25*, 1319–1322. [CrossRef]

22. Agrestini, S.; Metallo, C.; Filippi, M.; Campi, G.; Sanipoli, C.; De Negri, S.; Giovannini, M.; Saccone, A.; Latini, A.; Bianconi, A. Sc doping of MgB_2: The structural and electronic properties of $Mg_{1-x}Sc_xB_2$. *J. Phys. Chem. Solids* **2004**, *65*, 1479–1484. [CrossRef]

23. Ricci, A.; Poccia, N.; Campi, G.; Joseph, B.; Arrighetti, G.; Barba, L.; Reynolds, M.; Burghammer, M.; Takeya, H.; Mizuguchi, Y.; et al. Nanoscale phase separation in the iron chalcogenide superconductor $K_{0.8}Fe_{1.6}Se_2$ as seen via scanning nanofocused X-ray diffraction. *Phys. Rev. B* **2011**, *84*. [CrossRef]

24. Croft, T.P.; Lester, C.; Senn, M.S.; Bombardi, A.; Hayden, S.M. Charge density wave fluctuations in $La_{2-x}Sr_xCuO_4$ and their competition with superconductivity. *Phys. Rev. B* **2014**, *89*. [CrossRef]

25. Campi, G.; Innocenti, D.; Bianconi, A. CDW and similarity of the Mott insulator-to-metal transition in cuprates with the gas-to liquid- liquid transition in supercooled water. *J. Supercond. Nov. Magn.* **2015**, *28*, 1355–1363. [CrossRef]

26. Carlson, E.W. Condensed-matter physics: Charge topology in superconductors. *Nature* **2015**, *525*, 329–330. [CrossRef] [PubMed]

27. Giraldo-Gallo, P.; Zhang, Y.; Parra, C.; Manoharan, H.C.; Beasley, M.R.; Geballe, T.H.; Kramer, M.J.; Fisher, I.R. Stripe-like nanoscale structural phase separation in superconducting $BaPb_{1-x}Bi_xO_3$. *Nat. Commun.* **2015**, *6*. [CrossRef] [PubMed]

28. Campi, G.; Bianconi, A.; Poccia, N.; Bianconi, G.; Barba, L.; Arrighetti, G.; Innocenti, D.; Karpinski, J.; Zhigadlo, N.D.; Kazakov, S.M.; et al. Inhomogeneity of charge-density-wave order and quenched disorder in a high-Tc superconductor. *Nature* **2015**, *525*, 359–362. [CrossRef] [PubMed]

29. Campi, G.; Bianconi, A. High-Temperature Superconductivity in a Hyperbolic Geometry of Complex Matter from Nanoscale to Mesoscopic Scale. *J. Superconduct. Novel Magn.* **2016**, *29*, 627–631. [CrossRef]

30. Poccia, N.; Ricci, A.; Campi, G.; Caporale, A.-S.; Bianconi, A. Competing striped structures in La_2CuO_{4+y}. *J. Superconduct. Novel Magn.* **2012**, *26*, 2703–2708. [CrossRef]

31. Bianconi, A.; Lusignoli, M.; Saini, N.L.; Bordet, P.; Kvick, Å.; Radaelli, P.G. Stripe structure of the CuO_2 plane in $Bi_2Sr_2CaCu_2O_{8+y}$ by anomalous X-ray diffraction. *Phys. Rev. B* **1996**, *54*. [CrossRef]

32. Poccia, N.; Campi, G.; Fratini, M.; Ricci, A.; Saini, N.L.; Bianconi, A. Spatial inhomogeneity and planar symmetry breaking of the lattice incommensurate supermodulation in the high-temperature superconductor $Bi_2Sr_2CaCu_2O_{8+y}$. *Phys. Rev. B* **2011**, *84*. [CrossRef]

33. Caivano, R.; Fratini, M.; Poccia, N.; Ricci, A.; Puri, A.; Ren, Z.-A.; Dong, X.-L.; Yang, J.; Lu, W.; Zhao, Z.-X.; et al. Feshbach resonance and mesoscopic phase separation near a quantum critical point in multiband FeAs-based superconductors. *Superconduct. Sci. Technol.* **2009**, *22*. [CrossRef]

34. Bianconi, A. On the Fermi liquid coupled with a generalized Wigner polaronic CDW giving high T_c superconductivity. *Solid State Commun.* **1994**, *91*, 1–5. [CrossRef]

35. Fratini, M.; Poccia, N.; Ricci, A.; Campi, G.; Burghammer, M.; Aeppli, G.; Bianconi, A. Scale-free structural organization of oxygen interstitials in La_2CuO_{4+y}. *Nature* **2010**, *466*, 841–844. [CrossRef] [PubMed]

36. Zeljkovic, I.; Xu, Z.; Wen, J.; Gu, G.; Robert, S.M.; Hoffman, J.E. Imaging the Impact of Single Oxygen Atoms on Superconducting $Bi_{2+y}Sr_{2-y}CaCu_2O_{8+x}$. *Science* **2012**, *337*, 320–323. [CrossRef] [PubMed]

37. Zaanen, J. High-temperature superconductivity: The benefit of fractal dirt. *Nature* **2010**, *466*, 825–827. [CrossRef] [PubMed]

38. De Mello, E.V.L. Describing how the Superconducting Transition in La_2CuO_{4+y} is Related to the iO Phase Separation. *J. Superconduct. Novel Magn.* **2012**, *25*, 1347–1350. [CrossRef]

39. Kugel, K.I.; Rakhmanov, A.L.; Sboychakov, A.O.; Poccia, N.; Bianconi, A. Model for phase separation controlled by doping and the internal chemical pressure in different cuprate superconductors. *Phys. Rev. B* **2008**, *78*. [CrossRef]

40. Campi, G.; Innocenti, D.; Bianconi, A. CDW and similarity of the Mott Insulator-to-Metal transition in cuprates with the Gas-to-Liquid-liquid transition in supercooled water. *J. Superconduct. Novel Magn.* **2015**, *28*, 1355–1363. [CrossRef]

41. Bianconi, A. Quantum materials: Shape resonances in superstripes. *Nat. Phys.* **2013**, *9*, 536–537. [CrossRef]

42. Campi, G.; Dell'Omo, C.; Di Castro, D.; Agrestini, S.; Filippi, M.; Bianconi, G.; Barba, L.; Cassetta, A.; Colapietro, M.; Saini, N.L.; et al. Effect of temperature and X-ray illumination on the oxygen ordering in $La_2CuO_{4.1}$ Superconductor. *J. Superconduct.* **2004**, *17*, 137–142. [CrossRef]

43. Campi, G.; Di Castro, D.; Bianconi, G.; Agrestini, S.; Saini, N.L.; Oyanagi, H.; Bianconi, A. Photo-induced phase transition to a striped polaron crystal in cuprates. *Phase Trans.* **2002**, *75*, 927–933. [CrossRef]

44. Lausi, A.; Polentarutti, M.; Onesti, S.; Plaisier, J.R.; Busetto, E.; Bais, G.; Barba, L.; Cassetta, A.; Campi, G.; Lamba, D.; et al. Status of the crystallography beamlines at Elettra. *Eur. Phys. J. Plus* **2015**, *130*, 1–8. [CrossRef]

45. Achkar, A.J.; Zwiebler, M.; McMahon, C.; He, F.; Sutarto, R.; Djianto, I.; Hao, Z.; Gingras, M.J.P.; Hucker, M.; Gu, G.D.; et al. Nematicity in stripe-ordered cuprates probed via resonant X-ray scattering. *Science* **2016**, *351*, 576–578. [CrossRef] [PubMed]

46. Tabis, W.; Li, Y.; Tacon, M.L.; Braicovich, L.; Kreyssig, A.; Minola, M.; Dellea, G.; Weschke, E.; Veit, M.J.; Ramazanoglu, M.; et al. Charge order and its connection with fermi-liquid charge transport in a pristine high-T_c cuprate. *Nat. Commun.* **2014**, *5*. [CrossRef] [PubMed]

47. Comin, R.; Sutarto, R.; da Silva Neto, E.H.; Chauviere, L.; Liang, R.; Hardy, W.N.; Bonn, D.A.; He, F.; Sawatzky, G.A.; Damascelli, A. Broken translational and rotational symmetry via charge stripe order in underdoped $YBa_2Cu_3O_{6+y}$. *Science* **2015**, *347*, 1335–1339. [CrossRef] [PubMed]

48. Chen, X.M.; Thampy, V.; Mazzoli, C.; Barbour, A.M.; Miao, H.; Gu, G.D.; Cao, Y.; Tranquada, J.M.; Dean, M.P.M.; Wilkins, S.B. Remarkable stability of charge density wave order in $La_{1.875}Ba_{0.125}CuO_4$. *Phys. Rev. Lett.* **2016**, *117*. [CrossRef] [PubMed]